

Two Pathways for the Formation of Ethylene in CO Reduction on Single-Crystal Copper Electrodes

Klaas Jan P. Schouten, Zisheng Qin, Elena Pérez Gallent, and Marc T. M. Koper*

Leiden Institute of Chemistry, Leiden University, Einsteinweg 55, P.O. Box 9502, 2300 RA Leiden, The Netherlands

S Supporting Information

ABSTRACT: Carbon monoxide is a key intermediate in the electrochemical reduction of carbon dioxide to methane and ethylene on copper electrodes. We investigated the electrochemical reduction of CO on two single-crystal copper electrodes and observed two different reaction mechanisms for ethylene formation: one pathway has a common intermediate with the formation of methane and takes place preferentially at (111) facets or steps, and the other pathway involves selective reduction of CO to ethylene at relatively low overpotentials at (100) facets. The (100) facets seem to be the dominant crystal facets in polycrystalline copper, opening up new routes to affordable (photo)electrochemical production of hydrocarbons from CO₂.

The low-temperature reduction of carbon dioxide to hydrocarbons could be a very important step in a future sustainable carbon energy cycle.¹ Since the discovery by Hori et al.² in 1985, it has been known that CO₂ can be electrochemically reduced to methane and ethylene using copper electrodes. The formation of methane and especially ethylene is surprising and takes place to a significant extent only on copper electrodes. In spite of the extensive literature, the molecular mechanism is still unclear, in particular in relation to the C–C coupling step leading to the formation of ethylene. Understanding this C–C bond formation is important, as it would open up routes to the production of high-energy fuels by the (photo)electrochemical reduction of CO₂.

It is known that carbon monoxide is a key intermediate in CO₂ reduction and that methane and ethylene are formed from CO following different mechanisms.^{3–6} The central role of CO as the intermediate in the formation of such highly nontrivial products as methane and ethylene follows from the fact that CO is the only one-carbon molecule that gives the same product spectrum as CO₂ on a copper electrode, as documented in detail in the review by Hori.⁵ The formation of methane from CO depends on pH in such a way that the rate-determining step must involve the transfer of a proton and an electron.⁴ Recently, our own experiments⁷ as well as density functional theory (DFT) calculations by Peterson et al.⁸ suggested that the key intermediate in the formation of methane is CHO_{ads}. The formation of ethylene from CO, on the other hand, does not depend on pH.⁴ Therefore, a dimer of CO, whose formation does not involve the transfer of a hydrogen atom but does depend on potential (i.e., it involves

electron transfer), has been suggested as the key intermediate in the C–C coupling.^{6,7}

Hori et al.⁹ showed that the extent of methane and ethylene formation sensitively depends on the surface orientation of the copper electrode. On the (111) facet of the copper fcc crystal, the formation of methane is favored, whereas on the (100) facet, the formation of ethylene is dominant. Recent DFT calculations by Durand et al.¹⁰ predicted that the limiting potential for the formation of the intermediates of the CO₂ reduction to CH₄ is lower on the Cu(211) surface than on the Cu(111) and Cu(100) surfaces. No detailed DFT-based mechanism for the formation of ethylene was suggested, although these authors also considered CHO_{ads} as the intermediate in the formation of ethylene. Since the experiments by Hori et al. were carried out as long-term electrolysis experiments at a constant current, detailed information on the pathways of the C–C bond formation and its potential dependence is missing. Therefore, we report here our studies of the reduction of CO on two basal planes, Cu(111) and Cu(100), using online electrochemical mass spectrometry (OLEMS) to investigate the pathway to ethylene. This tip-based sampling technique allows the formation of volatile reaction intermediates and products to be followed while the potential at the electrode surface is changed, and it is similar to the differential electrochemical mass spectrometry (DEMS) technique.^{11–13} Experimental details concerning the preparation and characterization of the Cu single-crystal surfaces can be found in the Supporting Information (SI). We also note that for most of the measurements to be described below, the Faradaic current was mainly determined by hydrogen evolution and does not give much specific information about the CO reduction.

Figure 1 shows the reduction of CO on Cu(111) in pH 7 phosphate buffer (blue dotted lines with the current density and the mass signals on the left axis) and in pH 13 NaOH solution (green solid lines with the current density and the mass signals on the right axis). The potential was changed from 0 to –1 V and back at 1 mV/s. The recorded current is shown in the middle panel, and the volatile products measured during this potential scan are shown in the bottom panel. At –0.4 V, the current increased because of the formation of hydrogen at both pH 7 and 13 (although pH 13 appears to be more active for H₂ evolution). For all of the measurements performed, this current was mainly determined by hydrogen evolution and does not give any specific information about the CO reduction. The

Received: March 19, 2012

Published: June 6, 2012

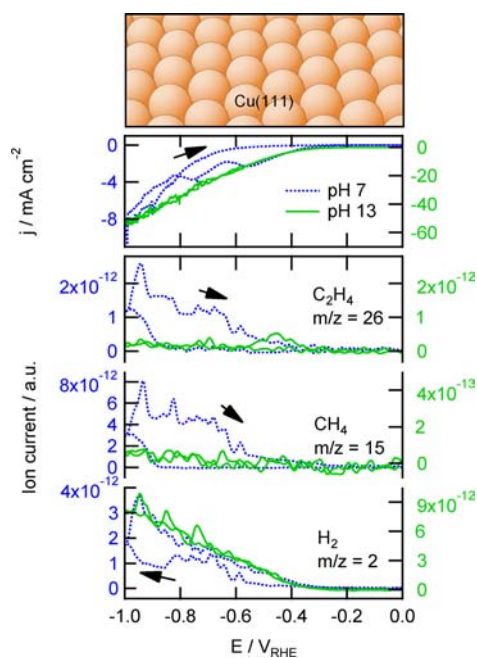


Figure 1. Top: (111) facet of the copper fcc crystal. Middle: cyclic voltammograms for the reduction of a saturated solution of CO (~ 1 mM) on Cu(111) in phosphate buffer (pH 7) and NaOH solution (pH 13). Bottom: associated mass fragments of volatile products measured with OLEMS. Data for pH 7 are shown with blue dotted lines and plotted against the left axis, and data for pH 13 are shown with green solid lines and plotted against the right axis.

hydrogen evolution led to the formation of gas bubbles trapped between the tip and the single-crystal electrode, which explains the somewhat noisy character of the observed mass signals. At pH 13, hardly any hydrocarbons were observed; only very small amounts of methane (represented by m/z 15, CH_3^+) and ethylene (represented by m/z 26, C_2H_2^+) were formed at the most negative potentials, as well as a very small amount of ethylene (but no methane) at -0.45 V. The latter is probably due to some (100) defects in the crystal, as can be concluded by comparing this to the results obtained on Cu(100) to be presented in Figure 2. At pH 7, both methane and ethylene were formed starting at -0.8 V, and both continued to be formed in the positive-going scan until -0.4 V. It should be noted that the potential dependence of the m/z 15 curve is very similar to that of the m/z 26 curve. One possible explanation for this similarity is that both masses are fragments of the same molecule. However, besides the mass fragments of methane and ethylene, we did not find other mass fragments with the same potential dependence, which shows that m/z 15 and 26 fragments come from different molecules. Therefore, we conclude that there must be a common (surface-adsorbed) intermediate in the reduction of CO (and hence CO_2) to CH_4 and C_2H_4 , since methane and ethylene are formed with the same potential dependence on Cu(111). We suggest that the hydrogenation of CO to form CHO_{ads} is the key step in the formation of both methane and ethylene on Cu(111). This conclusion agrees well with the calculations by Peterson et al., which indicated that for a stepped Cu(111) surface, “the key step in the formation of the hydrocarbons CH_4 and C_2H_4 is the hydrogenation of the adsorbed CO to form CHO_{ads} ”⁸.

The same experiments were done for a Cu(100) electrode, and the results are shown in Figure 2. The magnitude of the observed Faradaic current on Cu(100) was about twice as large

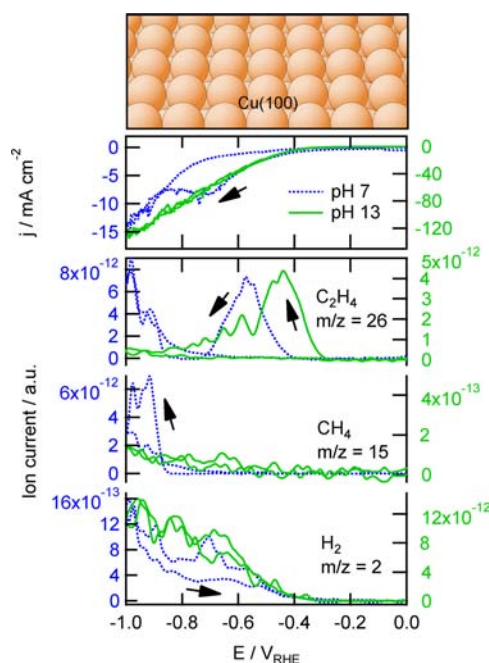


Figure 2. Top: (100) facet of the copper fcc crystal. Middle: cyclic voltammograms for the reduction of a saturated solution of CO (~ 1 mM) on Cu(100) in phosphate buffer (pH 7) and NaOH solution (pH 13). Bottom: associated mass fragments of volatile products measured with OLEMS. Data for pH 7 are shown with blue dotted lines and plotted against the left axis, and data for pH 13 are shown with green solid lines and plotted against the right axis.

as the current on Cu(111), which primarily reflects the enhanced ability of Cu(100) to catalyze hydrogen evolution.¹⁴ The observed hydrocarbon formation differed remarkably from that on Cu(111). Ethylene was already formed at potentials of -0.4 V at pH 7 and -0.3 V at pH 13. Ethylene formation exhibited maxima at -0.45 and -0.6 V, respectively, after which it decreased and eventually stopped. The current and charge corresponding to this peak of ethylene formation are too high to be explained by the reduction of a surface-adsorbed species. No methane was observed at these potentials. At a potential of -0.8 V at pH 7, the formation of ethylene was again observed, now accompanied by the formation of methane, similar to the simultaneous formation of CH_4 and C_2H_4 on Cu(111) at these potentials. This simultaneous formation of CH_4 and C_2H_4 below -0.8 V was not observed at pH 13 on Cu(100), in agreement with Cu(111) at this pH.

These results strongly suggest that there are two separate pathways for the formation of ethylene, one that shares an intermediate with the pathway to methane, as we observed on Cu(111) and below -0.8 V on Cu(100) at pH 7, and a second pathway that occurs only on Cu(100). For this second pathway, we suggest that the formation of a CO dimer is the key intermediate in the formation of ethylene. Such a surface dimer could explain the unique selectivity for ethylene (for detailed arguments, see ref 7) and is in agreement with the suggestion of Gatrell et al.,⁶ who proposed that this CO dimer would be more stable on Cu(100) surfaces.

As shown in Figure 2, we observed this ethylene formation only in the negative-going scan, as ethylene was not formed at potentials greater than -0.8 V in the positive-going scan. However, the ethylene formation was not permanently blocked. When we performed consecutive scans, we observed the same

potential dependence with ethylene formation in the negative-going scan, although the first scan always gave the highest activity (see Figure S2 in the SI). To investigate why ethylene was formed on Cu(100) only in the negative going scan at less-cathodic potentials, we performed consecutive scans of CO reduction at pH 13 on Cu(100) and increased the negative vertex potential with each scan; the results are shown in Figure 3. In the first scan (blue), the ethylene formation increased

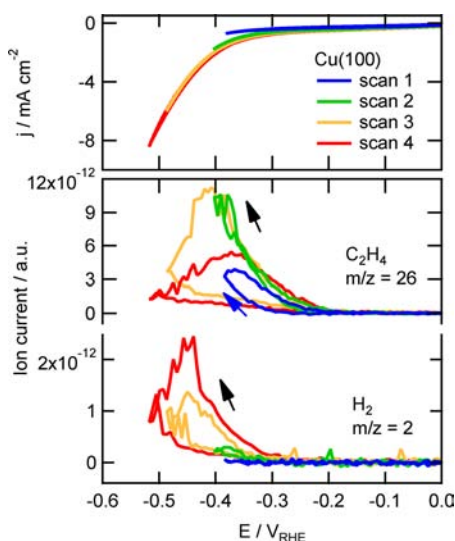


Figure 3. Consecutive scans of CO reduction with increasing cathodic potentials. Top: Cyclic voltammograms for the reduction of a saturated solution of CO (~ 1 mM) on Cu(100) in NaOH solution (pH 13). Bottom: associated mass fragments of volatile products measured with OLEMS.

when the potential was reversed at -0.38 V. In the second scan to -0.4 V (green), the ethylene formation was similar for the positive- and negative-going scans. In the third scan (yellow), the ethylene formation started to decrease below -0.42 V, and the ethylene formation in the positive-going scan was much lower than that in the negative-going scan. In the fourth scan (red), the ethylene formation was already lower in the negative-going scan. The hydrogen formation showed the opposite trend: there was no hydrogen formation in the first scan and only minor hydrogen formation in the second scan, and the hydrogen formation in the fourth scan was significantly larger than in the third scan. This is also reflected in the current, which increased from scan 1 to scan 4. These results clearly show that the deactivation is strongly potential-dependent. A possible explanation for these observations is reconstruction of the electrode surface. On Cu(100) in acidic media, a hydrogen-induced reconstruction with a concomitant increase in the hydrogen evolution reaction rate has been reported.¹⁵ Therefore, our observed increase in hydrogen formation and decrease in hydrocarbon formation could possibly be explained by such a reconstruction, but clearly, the details of this deactivation phenomenon remain to be understood. We also note that according to Hori et al.,¹⁶ the deposition of metal impurities from the electrolyte is the most common reason for deactivation. Given the partial reversibility of the deactivation phenomenon shown in Figure 3, we consider this explanation less likely, although we do not exclude that such effects may take place in our experiments on a longer time scale. One may also note that on Cu(111) the formation of methane and

ethylene was enhanced on the positive-going back scan (see Figure 1), suggesting potential-driven activation of the (111) surface, in contrast to the potential-driven deactivation of ethylene formation on Cu(100).

Figure 4 shows the results for similar experiments performed on a polycrystalline copper electrode. On this electrode, on

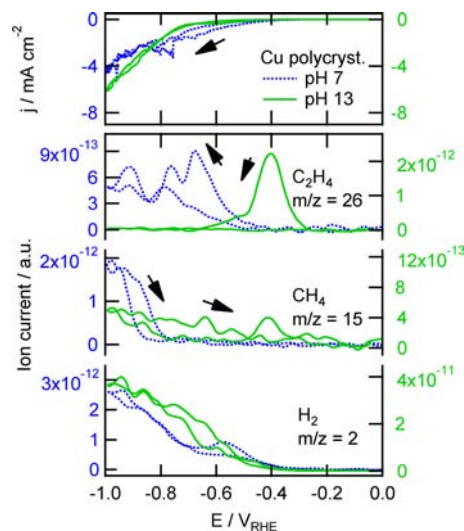


Figure 4. Top: Cyclic voltammograms for the reduction of a saturated CO solution (~ 1 mM) on polycrystalline copper in phosphate buffer (pH 7) and NaOH solution (pH 13). Bottom: associated mass fragments of volatile products measured with OLEMS. Data for pH 7 are shown with blue dotted lines and plotted against the left axis, and data for pH 13 are shown with green solid lines and plotted against the right axis.

which the various facets of the fcc crystal planes should be present, ethylene was formed at potentials of -0.5 V at pH 7 and -0.3 V at pH 13, similar to Cu(100). Also, the ethylene and especially methane formation below -0.8 V at pH 7 was very similar to that on Cu(100). The fact that the observed hydrocarbon formation on polycrystalline copper is similar to that on Cu(100) suggests that the dominant crystal facet on polycrystalline copper is the (100) facet. Such a conclusion has been drawn previously on the basis of blank voltammetry at copper in alkaline media.¹⁷

We note that our experiments at only two different pH values cannot accurately reflect the true pH dependence of the CO reduction. According to the results of Hori et al.,⁴ the formation of methane should take place at the same potential on the RHE scale at both pH 7 and pH 13. However, at pH 13, H₂ evolution was about an order of magnitude faster than at pH 7, presumably because of the absence of anions at pH 13,¹⁴ and this may suppress CO reduction. Clearly, the influence of pH and electrolyte composition, such as the presence of strongly adsorbing anions, requires further scrutiny. Furthermore, we note that because CO reduction currents are always low and also because hydrogen evolution close to the electrode leads to an effective stirring of the electrolyte, it is difficult to estimate any mass transport effects in relation to CO reduction.

To summarize, our experiments provide strong evidence for the idea that ethylene may be formed through two different mechanisms: one pathway has a common intermediate with the formation of methane and takes place on both the (111) and (100) surfaces, while in the second pathway, CO is selectively reduced to C₂H₄ at relatively low overpotentials, presumably

through the formation of a surface-adsorbed CO dimer.^{6,7} The latter pathway takes place preferentially at (100) facets. Moreover, the crystal plane at which this selective reduction to ethylene takes place, Cu(100), seems to be the dominant crystal facet in polycrystalline copper. These insights open up new routes to affordable (photo)electrochemical production of fuels from CO₂, especially because the selective ethylene formation pathway from CO has a remarkably low overpotential.

■ ASSOCIATED CONTENT

📄 Supporting Information

Experimental procedures and characterization of the copper single crystals, multiple scans of CO reduction, and ethylene formation at constant potential. This material is available free of charge via the Internet at <http://pubs.acs.org>.

■ AUTHOR INFORMATION

Corresponding Author

m.koper@chem.leidenuniv.nl

Notes

The authors declare no competing financial interest.

■ ACKNOWLEDGMENTS

This work was supported financially by the (Dutch) National Research School Combination - Catalysis (NRSC-C).

■ REFERENCES

- (1) Gattrell, M.; Gupta, N.; Co, A. *Energy Convers. Manage.* **2007**, *48*, 1255–1265.
- (2) Hori, Y.; Kikuchi, K.; Suzuki, S. *Chem. Lett.* **1985**, 1695–1698.
- (3) Hori, Y.; Murata, A.; Takahashi, R.; Suzuki, S. *J. Am. Chem. Soc.* **1987**, *109*, 5022–5023.
- (4) Hori, Y.; Takahashi, R.; Yoshinami, Y.; Murata, A. *J. Phys. Chem. B* **1997**, *101*, 7075–7081.
- (5) Hori, Y. *Mod. Aspects Electrochem.* **2008**, *42*, 89–189.
- (6) Gattrell, M.; Gupta, N.; Co, A. *J. Electroanal. Chem.* **2006**, *594*, 1–19.
- (7) Schouten, K. J. P.; Kwon, Y.; van der Ham, C. J. M.; Qin, Z.; Koper, M. T. M. *Chem. Sci.* **2011**, *2*, 1902–1909.
- (8) Peterson, A. A.; Abild-Pedersen, F.; Studt, F.; Rossmeisl, J.; Nørskov, J. K. *Energy Environ. Sci.* **2010**, *3*, 1311–1315.
- (9) Hori, Y.; Takahashi, I.; Koga, O.; Hoshi, N. *J. Mol. Catal. A: Chem.* **2003**, *199*, 39–47.
- (10) Durand, W. J.; Peterson, A. A.; Studt, F.; Abild-Pedersen, F.; Nørskov, J. K. *Surf. Sci.* **2011**, *605*, 1354–1359.
- (11) Gao, Y.; Tsuji, H.; Hattori, H.; Kita, H. *J. Electroanal. Chem.* **1994**, *372*, 195–200.
- (12) Baltruschat, H. *J. Am. Soc. Mass Spectrom.* **2004**, *15*, 1693–1706.
- (13) Wonders, A. H.; Housmans, T. H. M.; Rosca, V.; Koper, M. T. M. *J. Appl. Electrochem.* **2006**, *36*, 1215–1221.
- (14) Brisard, G.; Bertrand, N.; Ross, P. N.; Marković, M. N. *J. Electroanal. Chem.* **2000**, *480*, 219–224.
- (15) Matsushima, H.; Taranovskyy, A.; Haak, C.; Gründer, Y.; Magnussen, O. M. *J. Am. Chem. Soc.* **2009**, *131*, 10362–10363.
- (16) Hori, Y.; Konishi, H.; Futamura, T.; Murata, A.; Koga, O.; Sakurai, H.; Oguma, K. *Electrochim. Acta* **2005**, *50*, 5354–5369.
- (17) Droog, J. M. M.; Schlenter, B. J. *J. Electroanal. Chem. Interfacial Electrochem.* **1980**, *112*, 387–390.